Journal of Photochemistry and Photobiology A: Chemistry 219 (2011) 265–272

Contents lists available at ScienceDirect

Journal of Photochemistry and Photobiology A: Chemistry

journal homepage: www.elsevier.com/locate/jphotochem

Sulforhodamine B doped polymeric matrices: A high efficient and stable solid-state laser

Virginia Martín*, Angel Costela, Mercedes Pintado-Sierra, Inmaculada García-Moreno

Departamento de Sistemas de Baja Dimensionalidad, Superficies y Materia Condensada, Instituto de Química-Física "Rocasolano", CSIC, Serrano 119, 28006 Madrid, Spain

ARTICLE INFO

Article history:
Received 15 December 2010
Received in revised form 14 February 2011
Accepted 28 February 2011
Available online 5 March 2011

Keywords:
Solid-state dye lasers
Xanthenes dyes
Polymeric materials
Optoelectronic devices

ABSTRACT

We report the first systematic study on the laser action of Sulforhodamine B (SRB). Rhodamine B (RB), with similar molecular skeleton but with different phenyl substituents, was analysed to define the structural keystones in influencing their optical properties. Synthesis and laser characterization of photosensitized homopolymer, linear and crosslinked copolymers, and silicon-modified organic matrices were carried out. High lasing efficiencies, of up to 57%, were obtained with high photostability since the laser output remained stable, with no sign of photodegradation after 100,000 pump pulses at 10 Hz in the same position of the sample. These are, to the best of our knowledge, the topmost results achieved with new red-photosensitized materials to apply in advanced optical devices in this spectral region.

1. Introduction

In the development of solid state dye lasers, most of the work has been done using polymers [1,2] or silica gels [3,4] as host media. Initially, the sol–gel materials seemed to show higher photostability than those based in organic polymers, although refractive index inhomogeneities were a problem [5–7]. The use of synthetic polymers still presents additional advantages from both the technical and economic points of view: high optical homogeneity, better chemical compatibility with organic dyes, chemical versatility to change, in a controlled way, the final properties of the material (i.e., polarity, viscosity, molecular weight), high laser-radiation-damage threshold, inexpensive fabrication techniques which, combined with their light weight, facilitate both miniaturization and the design of integrated optical systems [8]. For these reasons, many efforts have been done to develop new photonic materials based on polymers doped with rare-earth-ions [9,10] as well as commercial [11] and newly synthesized dyes [12]. Up to date, the highest lasing efficiency and photostability from polymeric matrices doped with organic dyes has been recorded in the green-yellow region of the spectra [8]. Advanced optoelectronic and biophotonic applications require extending the wavelength-tuning emission of the dye-doped solid-state laser to the red part of the visible spectra.

Sulforhodamine B (SRB) and Rhodamine B (RB) (Fig. 1) are widely used laser dyes in the yellow-red spectral region, applied to generate femtosecond pulses in passive mode-locked, single-mode lasers amplifiers and hybrid mode-locked femtosecond lasers [13–15]. Proper understanding of the optical and spectroscopic properties of the RB and SRB dyes is complicated by the fact that these compounds exist in solution in a number of neutral and ionic forms [16]. Consequently, the properties of RB and SRB show great sensitivity to the solvent environment [17,18] and their photophysical properties have been extensively studied as a function of dye concentration, viscosity, polarity and polarizability of the solvents as well as the pH of the solution [13–27]: photophysics and photochemistry of RB and SRB depend not only on the solvent polarity [21–26] but also on the solvent viscosity [27,28] by the rotational motion of the *n*-diethyl groups around the xanthene amine bond. The data reported in these earlier works have been interpreted in different ways by different authors, leaving open the answer to the question onto which mechanism dominates the photodegradation process of these dyes [16,29–31]. Besides, no broad-based systematic studies have been carried out to analyse the photophysical influence on the laser behavior of RB and SRB [32–35].

In this paper, we present a careful analysis on the laser action of RB and SRB in relationship to chemical composition and macroscopic properties of the media into which they are incorporated. In addition, the present study is promoted by the similarity between RB and SRB, with the same xanthene skeleton but with different phenyl substituents, with the aim to identify which structural features are important in influencing the lasing properties of these dyes. Since the photophysical properties depend on environment, concentration of fluorophores and excitation conditions, we analyse first, the laser behavior of each dye in liquid phase, to proceed

* Corresponding author.
E-mail address: vmartin@iqfr.csic.es (V. Martín).

1010-6030/$ – see front matter © 2011 Elsevier B.V. All rights reserved.
doi:10.1016/j.jphotochem.2011.02.030

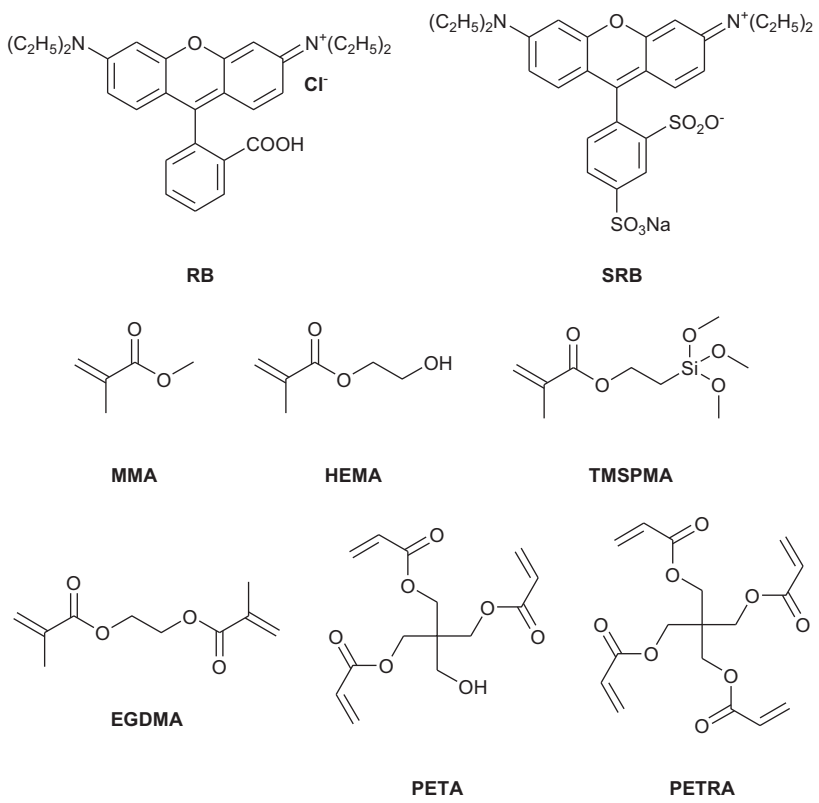

Fig. 1. Molecular structures of Rhodamine B (RB) and Sulforhodamine B (SRB) dyes as well as the monomers selected in this work: methyl methacrylate (MMA), 2-hydroxyethyl methacrylate (HEMA), 3-(trimethoxysilyl)propyl methacrylate (TMSPMA), ethylene glycol dimethacrylate (EGDMA), pentaerythritol triacrylate (PETA), and pentaerythritol tetraacrylate (PETRA).

then to a thorough study in solid matrices. Taking into account that the laser action of RB and SRB in solid-state materials has been scarcely studied [32–40], the present work represents, to the best of our knowledge, the first systematic study on the solid-state laser action of these dyes doped organic and hybrid matrices. Among the almost unlimited possible compositions and structures of solid materials to be doped with laser dyes, the liquid-phase analysis guides the selection of the best dye/host matrix in order to optimize the laser action attending to both lasing efficiency and photostability. Attention has been paid to the influence of the crosslinking degree of the materials on the laser action, since the well known effect of cage confinement on molecular motions could enhance the photostability of the encapsulated dye molecules in solid state [41–43]. More importantly, the substituents in the phenyl ring of these dyes could provide an excellent opportunity to analyse the effect of hydrogen bonding inside different polymer environments. The SRB-doped materials herein synthesized are found to be the most efficient and photostable solid-state laser dyes recorded up to now with emission at ca. 600 nm.

2. Experimental

2.1. Materials

Rhodamine B (chloride salt) and Sulforhodamine B (laser grade, Exciton) were used as received with a purity >99% (checked by spectroscopic and chromatographic methods). Solvents for laser studies were of spectroscopic grade (Merck, Aldrich or Sigma) and were used without purification. Linear copolymers were obtained by copolymerization of 2-hydroxyethyl methacrylate (HEMA) with different volumetric proportions of methyl methacrylate (MMA) and of the sililated monomer 3-(trimethoxysilyl)propyl methacrylate (TMSPMA). Crosslinked matrices were obtained by copolymerization of HEMA/MMA with monomers with more than one polymerizable double bond per molecule. Di-, tri- and tetra-functionalizated comonomers, such as ethylenglycol dimethacrylate (EGDMA), pentaerythritol triacrylate (PETA) and pentaerythritol tetraacrylate (PETRA), respectively, were selected. All monomers were purchased from Aldrich. MMA, HEMA and TMSPMA were purified by distillation prior to use while EGDMA, PETA and PETRA were used as received. Fig. 1 shows the molecular structures of these monomers.

2.2. Preparation of solid polymeric samples

Sulforhodamine B was incorporated into the different solid matrices following the procedure previously described [44]. The solid monolith laser samples were cast in a cylindrical shape, forming rods of 10 mm diameter and 10 mm length. A cut was made parallel to the axis of cylinder to obtain a lateral flat surface of $\approx$6 mm $\times$ 10 mm. This surface as well as the ends of the laser rods were prepared for lasing experiments by using a grinding and polishing machine (Phoenix Beta 4000, Buehler) until optical-grade finished. The planar ground stage was carried out with a Texmet 1000 sand paper (Buehler) using a diamond polishing compound of 6 μm as an abrasive in mineral oil as a lubricant. The final polished stage was realized with a G-Tuch Microcloth (Buehler), using a cloth disk Mastertex (Buehler) with diamond of 1 μm in mineral oil as an abrasive type.

2.3. Methods

Lasing efficiencies and photostabilities were evaluated in a simple plane–plane oscillation cavity consisted of a 90% reflectivity

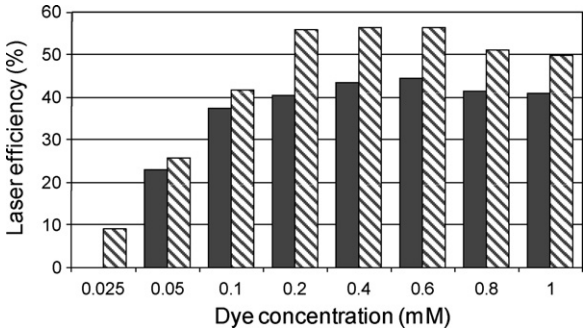

Fig. 2. Lasing efficiency of RB (dark column) and SRB (dashed column) as a function of the dye concentration in ethanol.

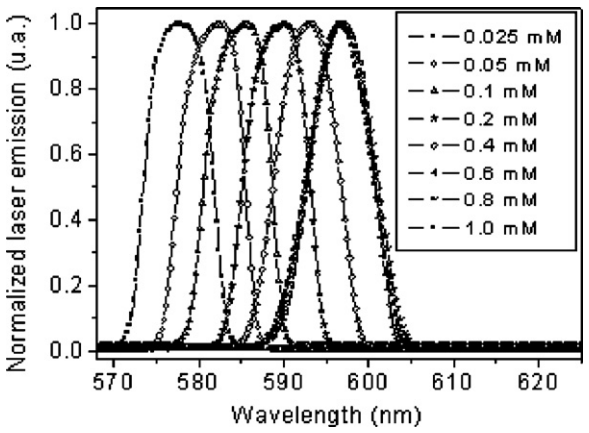

Fig. 3. Lasing emission spectra of dye SRB as a function of the dye concentration in ethanol.

aluminium mirror and the end face of the cell (or sample) as the output coupler. Liquid solutions of dyes were contained in 1 cm optical-path quartz cells that were carefully sealed to avoid solvent evaporation during experiments. Both the liquid cells and the solid samples were transversely pumped at 532 nm with 5.5 mJ, 6 ns FWHM pulses from a frequency-doubled Q-switched Nd:YAG laser (Monocrom OPL-10) at a repetition rate of up to 10 Hz. The reflectivities of the sample faces at the lasing wavelength were estimated to be 4%. Details of the experimental system can be found elsewhere [45].

Narrow-line-width laser emission and tuning ranges of dye solutions were obtained by placing the samples in a home-made Shoshan-type oscillator [46], consisting of full-reflecting aluminium back and tuning mirrors and a 2400 lines mm^{-1} holographic grating in grazing incidence, with outcoupling via the grating zero order. Wavelength tuning was accomplished by rotation of the tuning mirror. Tuning mirror and grating (both from Optometrics) were 5 cm wide and the angle of incidence on the grating was 88.5°. Laser line width was measured with a Fabry–Perot etalon (IC Optical Systems) with a free spectral range of 15.9 GHz.

3. Results and discussion

3.1. Lasing properties in liquid phase

Firstly, we carried out a systematic analysis of the laser behavior of the selected red-edge dyes in liquid phase as a guide to develop polymeric materials which could enhance their laser action in solid-state. The dependence of the laser action on the concentration of both dyes was analysed in ethanol. The experiments were performed increasing the dye concentration while other experimental parameters were kept constant. Dye solutions with optical densities (for 1 cm path length) in the range 1.5–30 were prepared and their lasing properties evaluated.

The lasing efficiencies of both dyes, defined as the ratio between the energy of the dye laser output and the energy of the pump laser incident on the sample surface, as a function of the dye concentration are reported in Fig. 2. As it was expected, for all the analysed solutions their lasing efficiencies increase significantly with the dye concentration until a maximum value is reached in solutions with optical density of ca. 18. From this point on, further increases in the dye concentration do not increase lasing efficiency, which begins to slight decrease.

The laser spectra of both dyes exhibit the same dependence on the dye concentration. For this reason, and for the sake of clarity, only the emission spectra of SRB are shown in Fig. 3. The laser spectrum is shifted to lower energies as the concentration increases. This trend is related to the effect of reabsorption/reemission phenomena on the emission intensity, because the possibility of exciting molecules by absorption of a photon previously emitted by another molecule in the medium depends on the overlapping between absorption and fluorescence spectra, which is affected by the dye concentration [47]. Reabsorption/reemission effects could explain the apparent decrease of the lasing efficiencies observed at high dye concentrations.

The actual effect of the solvent on the lasing emission of dyes RB and SRB was analysed at a common concentration (6×10^{-4} M), the one that optimizes the lasing action of both dyes in ethanol. Since the optimum efficiency in different solvents could occur at different concentrations it was verified that this effect was not pronounced in the selected media. Table 1 summarizes the laser properties of these dyes in several solvents, although their low solubility in polar non-protic and apolar ones, such as cyclohexane and ethyl acetate, prevents attaining the necessary high concentrations required under the pumping conditions selected in the present work. The polar protic nature of the solvents improves the lasing efficiency of both dyes.

The laser action of these chromophores is significantly affected by the influence of the pendant substituents on the hydrogens of the xanthene group [48]. RB emits laser radiation more efficiently than SRB probably due to the stabilization of its ionic form in protic solvents by hydrogen bonding (presumably at the COO– group), whereas the non-fluorescent lactonic structure of RB is present in aprotic solvents as acetone [18]. The capability to stabilize the zwitterions decreases in alcohols with longer hydrocarbon chain lengths [18], reducing the lasing efficiency of RB until a value similar to that registered with SRB.

The lasing photostability of both dyes was analysed under identical experimental conditions to those selected to irradiate the fluorophores when embedded in solid polymeric matrices, which will allow comparison, in due time, of their stability in both liquid and solid phases under laser irradiation. Because the irradiated volume in solid samples under the selected experimental conditions

Table 1
Laser parameters[a] for RB and SRB dyes in different solvents. Nd:YAG laser (second harmonic) pump energy: 5.5 mJ/pulse. Dye concentration: 6×10^{-4} M.

Solvent	RB		SRB	
	Eff (%)	λ_{max}(nm)	Eff (%)	λ_{max} (nm)
F_3-ethanol[b]	58	592	40	596
Methanol	57	597	52	599
Ethanol	53	598	51	597
Acetone	41	598		

[a] Eff: energy conversion efficiency; λ_{max}: peak wavelength of the laser emission.
[b] F_3-ethanol: 2,2,2-trifluoroethanol.

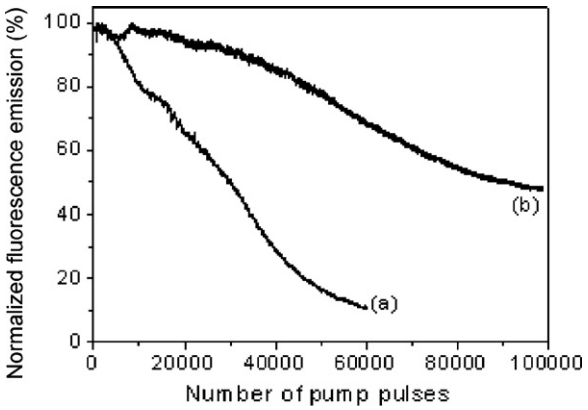

Fig. 4. Normalized laser-induced fluorescence emission as a function of the number of pump pulses at 10 Hz repetition rate for the dyes RB (a) and SRB (b) in ethanolic solutions.

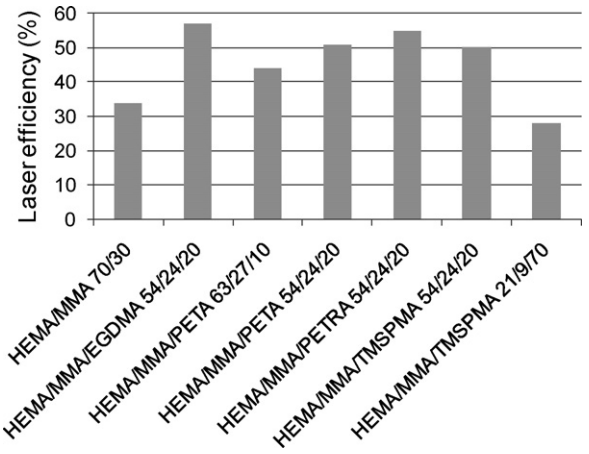

Fig. 5. Influence of the matrix composition on the laser efficiency of SRB incorporated in some of the synthesized samples (data from Table 2).

was estimated to be 10 μL, capillary tubes (1 cm height, 1 mm internal diameter) into which ethanolic solutions were incorporated offer the best geometry to produce an irradiated volume similar to that analyse in the solid samples, thus maintaining the same laser pump conditions in both cases.

Although the optical quality of the capillary prevents laser emission from the dyes, information about their photostabilities can be obtained following the decrease in the laser-induced fluorescence intensity, excited transversally to the capillary, as a function of the number of pump pulses. The fluorescence emission was monitored perpendicular to the exciting beam, and its collection and analysis were carried out with the same set-up selected to characterize the laser emission from dyes incorporated into solid samples. The concentration of the dyes was 6×10^{-4} M so that both samples had the same optical density at 532 nm (OD ≈ 18). The results obtained from the dyes RB and SRB are plotted in Fig. 4. Gradual decrease in the output energy, due to the progressive photo- and thermodegradation of the dye molecules, was observed in both dyes. This decrease occurred with a faster rate in the case of RB where after 60,000 shots the output energy dropped to 9% of its initial value, compared to a drop to only 72% in the case of SRB.

Although no photobleaching study of SRB and RB has been previously reported [30], some details of competitive pathways of the photodegradation mechanism of these dyes can be inferred from previous experimental data [49–51]. Thus, it has been established that the photostability of rhodamine fluorophores is essentially determined by both specific interactions of their amine groups with the environment and generation of free radicals from the substituents in the phenyl groups [52].

The capability of the carboxyphenyl group of RB to form hydrogen bonds in protic media such as ethanol is expected to result in lower photostability because of increased dynamic interactions with solvent molecules [30]. In addition, the faster degradation of RB with respect to SRB could be related to differences in two photophysical parameters: first, the absorption coefficient for the S_n–S_1 process in SRB is lower than the corresponding in RB [28] and secondly, the energy separation between S_1 and T_1, which may predict the relative magnitude of the rate of intersystem crossing and triplet lifetime, of SRB is higher than that of RB [32].

3.2. Lasing properties in solid-state

As the studies in liquid phase showed that both dyes, RB and SRB, exhibited similar lasing efficiencies but dye SRB has higher photostability under the selected pump conditions, the influence of both composition and structure of the solid matrix on the laser action was only studied, in a systematic way, for this dye (Fig. 5). With this aim, a number of polymeric formulations with different plasticity and/or degree of crosslinking were synthesized as host materials for the SRB dye. The actual composition of these materials was decided in the light of the information obtained in our previous studies of the lasing action of dyes dissolved in different organic and hybrid solid materials [36,44,53,54]. The dye concentration was selected to be 6×10^{-4} M because that was one of the concentrations producing the highest efficiencies in liquid solution.

Broad-line-width laser emission in a simple plane–plane nontunable resonator with emission peaked at ca. 605 nm, beam divergence of ≈5 mrad, energy threshold of 0.8 mJ, and pulse duration of ≈5 ns FWHM, was obtained from the materials under study. The tuning capability of the dye-doped solid matrices, one of the most important features of dye lasers, was determined placing the samples in a grazing-incidence grating cavity in Shoshan configuration. Tunable laser emission with line width of the order of 0.15 cm^{-1} was obtained, with a tuning range of 65 nm, from 580 to 645 nm.

3.2.1. Laser operation in linear copolymers

In solid samples, the polarity of the polymeric medium can be modulated by working with appropriate copolymers. As was discussed above, improvements in the lasing properties of SRB were found with solvents such as ethanol defining a protic medium. Thus, a monomer functionalized with polar groups, such as HEMA, was chosen as the pivotal component in the formulations since it mimics ethanol. Copolymers of HEMA with MMA were prepared in volumetric proportions ranging from 100/0 (PHEMA homopolymer) to 50/50.

The results obtained are summarized in Table 2. The laser emission spectra of these linear copolymers was centered at ca. 605 nm, bathochromically shifted by ca. 10 nm with respect to those registered in liquid phase even for dye concentrations higher than that selected to dope these polymeric matrices. This behavior agrees with the observed red-shifted of the absorption and fluorescence peaks of xanthenes with similar molecular structure as the viscosity of the medium increases [16,29].

Lasing efficiencies of ca. 32% were obtained in these linear copolymers with independence of their composition. These efficiencies are lower than those registered in liquid phase. In this regard, it has to be taken into account that the final surface roughness is limited by the employed material as polishing. In our case, the final polished treatment is carried out with a suspension of diamond (1 μm) in mineral oil, so the attained surface roughness is around 500 nm, very far from the laser-grade polishing (λ/10).

Table 2
Laser parameters[a] for SRB dye in linear, crosslinked and silicon-containing organic matrices. Nd:YAG (second harmonic). Pump energy: 5.5 mJ/pulse. Repetition rate: 10 Hz. Dye concentration: 6×10^{-4} M.

Material	Eff (%)	λ_{max} (nm)	$I_{100,000}$ (%)[b]	$I_{100,000}$ (%)[d]
PHEMA	32	604	(21)[c]	
COP(HEMA/MMA 80/20)	32	604	(21)[c]	
COP(HEMA/MMA 70/30)	34	605	20	
COP(HEMA/MMA 50/50)	32	609	18	
TER(HEMA/MMA/EGDMA 63/27/10)	56	605	59	80
TER(HEMA/MMA/EGDMA 56/24/20)	57	604	51	32
TER(HEMA/MMA/EGDMA 49/21/30)	48	609	13	(20)[c]
TER(HEMA/MMA/PETA 63/27/10)	44	606	(25)[c]	31
TER(HEMA/MMA/PETA 56/24/20)	51	608	44	63
TER(HEMA/MMA/PETA 49/21/30)	52	608	69	82
TER(HEMA/MMA/PETRA 63/27/10)	46	609	35	99
TER(HEMA/MMA/PETRA 56/24/20)	55	608	53	69
TER(HEMA/MMA/PETRA 49/21/30)	49	606	33	
TER(HEMA/MMA/TMSPMA 63/27/10)	43	605	33	
TER(HEMA/MMA/TMSPMA 56/24/20)	50	605	44	
TER(HEMA/MMA/TMSPMA 49/21/30)	38	605	45	
TER(HEMA/MMA/TMSPMA 35/15/50)	35	605	(21)[c]	
TER(HEMA/MMA/TMSPMA 28/12/60)	31	606	(20)[c]	
TER(HEMA/MMA/TMSPMA 21/9/70)	28	601	(5)[c]	

[a] As defined in Table 1.
[b] Intensity of the dye laser output after 100,000 pump pulses in the same position of the sample referred to the initial intensity I_0, $I_n(\%) = (I_n/I_0) \times 100$.
[c] Intensity of the dye laser output after 50,000 pump pulses.
[d] Influence of the postpolymerization thermal treatment on the laser photostability.

The lasing stability was studied by following the evolution of the laser emission with the number of pump pulses in the same position of the sample at 10 Hz repetition rate. Values of the laser output normalized to the initial lasing intensity after 100,000 pump pulses in the same position of the sample are collected in Table 2. To facilitate comparison, some of these data have been represented graphically in Fig. 6. Contrary to the efficiency behavior, the lasing photostability depends strongly on the composition of the matrix since the presence of MMA increases significantly the lasing lifetime. The best photostability and the highest lasing efficiency are attained with SRB dissolved in the copolymer COP(HEMA/MMA 70/30). As the proportion of MMA increases in the matrix the internal plasticization decreases, the polymer becomes more rigid, the protecting "polymer cage" that surrounds the dye groups strengthens and, as a result, the chromophore could be less bleached [52]. Consequently, increasing the rigidity of the matrix by copolymerization with crosslinked monomers could be of utmost importance in order to improve the laser action of SRB incorporated into solid materials.

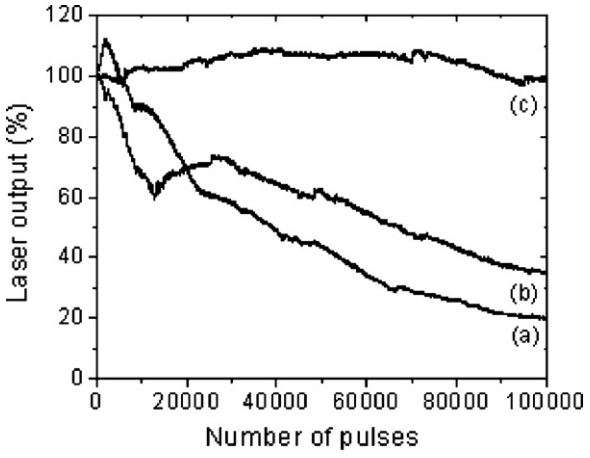

Fig. 6. Normalized laser output as a function of the number of pump pulses for SRB dye dissolved in (a) copolymer (HEMA/MMA 70/30), (b) crosslinked tertpolymer TER(HEMA/MMA/PETRA 63/27/10) and (c) same tertpolymer thermally postcured. Dye concentration: 6×10^{-4} M. Pump energy and repetition rate: 5.5 mJ/pulse and 10 Hz, respectively.

In addition, HEMA monomer could interact, to some extent, through hydrogen bonding with SRB molecules, not only influencing dye mobility but also increasing dynamic interactions between guest molecule and its surrounding polymer chains. Because of enhanced dye–polymer interactions, the photophysical properties of the dye could be potentially altered and, consequently, laser efficiency will be reduced and photodegradation will be most likely to occur.

3.2.2. Laser operation in crosslinked copolymers

Methacrylic (EGDMA) and acrylic (PETA, PETRA) crosslinking monomers, with different numbers of polymerizable groups per monomer molecule, were chosen for preparing three-dimensional crosslinked matrices based on the copolymer (HEMA/MMA 70/30) that optimized the laser action of SRB dissolved in linear polymers, the crosslinked monomer was added in a ratio from 10 to 30% with respect to the total amount of the linear copolymer. EGDMA is a double functionalized monomer (two double bonds), PETA is triple functionalized (three double bonds) and PETRA is quadruple functionalized (four double bonds).

The lasing results obtained with SRB dye solved in the different crosslinked polymers are summarized in Table 2. Comparison with the results exhibited by the dye incorporated into linear copolymers, shows that the crosslinking does not affect significantly the peak wavelength of the emission band but enhances drastically the lasing efficiencies. Values of efficiency up to 57% were registered, which are higher than those recorded in liquid phase, in spite of the grinding and polishing of the solid samples not being laser grade, which as these solid materials. This result agrees with the previously observed increase of fluorescence quantum yield of SRB with the viscosity of the media, which was correlated with a decrease of the internal conversion rate associated to the rotation of the diethyl-amino groups around the xanthene amine bonds [29]. In the crosslinked matrices, the micro-viscosity is very high and hence the immobilization of the dye leaded to a significant increase of the laser efficiency. Although the viscosity effect could also be present in the lineal matrices, its positive contribution to the laser action of SRB could be reduced because, in the HEMA/MMA copolymers, it competes with the mentioned dye–polymer interactions by hydrogen bonds.

The photostability of SRB dye doped crosslinked matrices also increases significantly with respect to those registered in the linear polymers. Thus, the laser emission of the dye doped in TER(HEMA/MMA/PETA 49/21/30) material remains at to 69% of its initial value after 100,000 pump pulses in the same position of the sample. The photostability of the dye depends strongly on both the composition and the structure of the matrix, existing for each functionalized monomer a volumetric proportion that optimizes the laser action of SRB.

Taking into account the high proportion as well as the high functionalization degree of these crosslinking monomers, the presence of residual free double bonds that remain into the matrices due to the soft thermal conditions selected to carry out the polymerization could induce photobleaching reactions of dye molecules. In a further attempt to improve the photostability of the laser output, some crosslinked samples were subjected to a postpolymerization thermal treatment in order to induce a higher polymerization degree of the residual double bounds. This thermal treatment consisted basically of a small increase of temperature, from 30 to 95 °C, during seven days, and the posterior decreasing of it to room temperature at a rate of 5 °C/h. The lasing photostability of the dye doped the samples thermally treated are also reported in Table 2. As can be seen, with the exception of terpolymer with 20 and 30% of EGDMA, the lasing lifetime of SRB solved in the thermally postcured samples significantly improves the previous results, being this effect especially remarked in matrices with higher proportion and functionalization of the crosslinking monomer. Thus, after this thermal treatment, the laser action of SRB solved in the tertpolymer (HEMA/MMA/PETRA 63/27/10) remains stable, with no sign of degradation after 100,000 pump pulses at 10 Hz in the same position of the sample. However, further increases in the proportion of PETRA result in a decrease of photostability.

Although the photostability behavior of the dye as a function of the material's degree of crosslinking does not follow a defined pattern, the high lasing lifetime recorded in these matrices points to the importance of the proper adjustment of the rigidity of the polymer on the laser performance of dyes. For a certain crosslinking degree, the free volume available within the polymeric matrix will be completely occupied by the dye. Increasing the degree of crosslinking beyond this point will result in the dye molecules being partially excluded from the shrinking free volume, and formation of dimers and/or reactions with other species, impairing the laser operation, will be forced. In the present case, the results obtained indicate that to optimize the photostability of SRB the crosslinking monomer must be tetra functionalized such as PETRA, and must be added in volumetric proportions up to 10% with a supplemental thermal treatment to induce the polymerization of the residual double bonds. Consequently, the development of solid-state dye lasers based on crosslinked matrices requires a very careful optimization of the thermal conditions selected to carry out the final polymerization of the material in order to reduce the presence of residual monomer and free double bonds without inducing the thermal degradation of the dye molecules.

As discussed above, the enhancement of the laser action of SRB doped crosslinked matrices should be credited mainly to the effect of the cage confinement on molecular motions and interactions. In fact, the incorporation of fluorophores into nano- and micrometer-sized organic and inorganic particles is a strategy of increasing importance [55–61] to circumvent the often undesired sensitivity and interactions of most chromophores to their local environment (i.e. self-quenching or aggregation), which are of the most important effects present in organic dyes affecting their colour, solubility and photophysical properties. But also, for a polar dye such as SRB, its cage confinement could have an additional effect leading also to an increase of its laser action. A multiply charged molecule like SRB has a strong dipole moment that is capable of arranging surrounding solvent molecules into a highly directional solvation shell, generating a polarization field that is constantly being disrupted, and hence weakened, by random molecular motions in bulk solutions. However, under the confinement imposed by the crosslinked matrices, the polarization field of the solvation shell will be weakened to a lesser extent, due to a reduction of the random molecular motions and to less polar media relative to solvents like ethanol [62–64]. As a result of a stronger polarization field, molecular motions surrounding SRB would be impaired and solvation dynamics would be slower than that observed in bulk liquids.

3.2.3. Laser operation in silicon-containing organic matrices

Silicon-containing polymer matrices have the advantage of remaining organic, which means plasticity and an easy synthesis procedure, but with improved thermal properties due to the presence of the silicon atoms in their structure. Previous studies revealed that the laser action of dyes properly incorporated into silicon-modified organic matrices could be greatly enhanced [53,54].

Trying to improve further the laser action of SRB in solid materials, this dye was incorporated into terpolymer of (HEMA/MMA 70/30) with TMSPMA added in volumetric proportions ranging from 10 to 60%, with respect to the total amount of the former copolymer. Taking into account that there is one silicon atom per TMSPMA monomer repetition unit, which appears as side substituent (see Fig. 1) the concentration of silicon atoms varies from 1% in the terpolymer (HEMA/MMA/TMSPMA 63/21/10) to 7% in the formulation (HEMA/MMA/TMSPMA 28/12/60). The lasing results obtained are collected in Table 2. Comparison of the data summarized in this table shows that the laser performance of SRB dye incorporated into organic matrices with content of the sililated monomer up to 30%, improves that reached in the linear copolymers but worsens the exhibited in some of the synthesized crosslinked matrices. Further increase in the proportion of the sililated monomer leads to a significant decrease of the SRB laser action. In fact, the glass transition temperature of these sililated materials decreases as the proportion of monomer TMSPMA in the matrix increases [54], reflecting the plasticizer effect of the alkoxides groups with a lessening in the laser action, as was discussed above.

Although the photobleaching of dyes can occur by several different mechanisms and, from a general point of view, can be considered to be quite complex, at low irradiances and under ambient atmosphere the primary photodegradation event of rhodamines is believed to be photo-oxidation. In fact, all xanthene dyes exhibit higher photostability in an oxygen-depleted atmosphere, pointing to the role of photo-oxidation in a single-photon photobleaching process. As a result, factors that accelerate oxygen diffusion, such as the higher oxygen permeability in sililated materials and the longer lifetime of singlet molecular oxygen in these media [65], are expected to reduce the SRB photostability and may help to explain the shorter lifetime found in the sililated samples

4. Conclusions

In this paper we report the first systematic study on the laser action of two fluorophores, RB and SRB, with similar molecular skeleton but with different phenyl substituents, related to the macroscopic properties of the media into which they are incorporated. The obtained experimental data show the extreme relevance of the phenyl pending group in chemical interactions of these dyes with the solvent system, which determined a higher photostability for the sulfonated derivative under transversal pumping conditions at 532 nm.

Efficient and photostable laser operation of SRB has been demonstrated when the dye was incorporated into polymeric matrices based on linear, crosslinked with different degrees of functionalization, and silicon-containing copolymers. Under transversal pumping in non-optimized laser cavities the laser action of SRB resulted optimized in organic matrices based on a tetra-functionalized crosslinked monomer such as PETRA, added in volumetric proportion up to 10%, and with a supplemental thermal treatment to induce the polymerization of the residual double bonds. Thus, high lasing efficiencies, up to 57%, were obtained with high photostability, with the laser output remaining stable after 100,000 pump pulses at 10 Hz in the same position of the sample. Cage confinement of SRB into a crosslinked matrix protected the dye molecules and restricted their molecular motions resulting in enhancement of laser action as compared with the effect of hydrogen bonding to lock the dye in linear polymers based on acrylic monomers such as HEMA. The crosslinked copolymers are demonstrated to be the best host media for tunable solid-state lasers emitting in this red-edge spectral region. These new laser materials have the potential to be used as active media in highly processible, reproducible, versatile, and easy to handle solid-state dye lasers replacing in some applications the available dye lasers in liquid phase.

The materials described in this work and their utilization in solid-state dye lasers are covered by Spanish Patent No. P200802558 filed on September 2008.

Acknowledgements

This work was supported by Project MAT2010-20646-C04-01 of the Spanish CICYT. V. Martín thanks CSIC for her JAE-postdoctoral contract. M. Pintado-Sierra acknowledges a research grant from MICINN (cofinanced by Fondo Social Europeo).

We want to dedicate this paper in memoriam to Prof. Roberto Sastre, who passed away on 27th February. Prof. Sastre was an outstanding and innovative researcher on the photochemistry of polymers and synthesis of new organic and organic-inorganic hybrid materials. He was cheerful and enthusiastic in his work and was beloved by students and colleagues. All of us will greatly miss him.

References

[1] S.M. Giffin, W.J. Wadsworth, I.T. McKinnie, A.D. Woolhouse, G.J. Smith, T.G. Haskell, Efficient, high photostability, high brightness, co-polymer solid state dye lasers, J. Mod. Opt. 46 (1999) 1941–1945.
[2] G.M. Wang, Z.H. Zhang, Solid-state dye lasers based on polymethyl methacrylate doped with Pyrromethene 650, Laser Phys. 20 (2010) 1865–1867.
[3] R. Reisfeld, Stable visible lasers based on sol gel technology, Ceramic Transactions, Sol–Gel Sci. Technol. 55 (1995) 317–329.
[4] C. Sanchez, B. Lebeau, F. Chaput, J.P. Boilot, Optical properties of functional hybrid organic–inorganic nanocomposites, Adv. Mater. 15 (2003) 1969–1994.
[5] J.C. Altman, P.E. Stone, B. Dunn, F. Nishida, Solid-state laser using a rhodamine-doped silica gel compound, IEEE Photon. Tech. Lett. 3 (1991) 189–190.
[6] F.J. Duarte, Solid-state multiple-prism grating dye–laser oscillators, Appl. Opt. 33 (1994) 3857–3860.
[7] I. García-Moreno, A. Costela, A. Cuesta, O. García, D. del Agua, R. Sastre, Synthesis, structure, and physical properties of hybrid nanocomposites for solid-state dye lasers, J. Phys. Chem. B 109 (2005) 21618–21626.
[8] F.J. Duarte (Ed.), Tunable Laser Applications, CRC Press, Atlanta, 2008.
[9] C. Grivas, J. Yang, M.B.J. Diemeer, A. Driessen, M. Pollnau, Continuous-wave Nd-doped polymer lasers, Opt. Lett. 35 (2010) 1983–1985.
[10] J. Yang, M.B.J. Diemeer, C. Grivas, G. Sengo, A. Driessen, M. Pollnau, Steady-state lasing in a solid polymer, Laser Phys. Lett. 7 (2010) 650–656.
[11] Y. Yang, R. Goto, S. Omi, K. Yamashita, H. Watanabe, M. Miyazaki, Y. Oki, Highly photo-stable dye doped solid-state distributed-feedback (DFB) channeled waveguide lasers by a pen-drawing technique, Opt. Express 18 (2010) 22080–22089.
[12] J. Bañuelos-Prieto, A.R. Agarrabeitia, I. García-Moreno, I. López-Arbeloa, A. Costela, L. Infantes, M.E. Pérez-Ojeda, M. Palacios-Cuesta, M.J. Ortíz, Controlling optical properties and function of BODIPY by using asymmetric substitution effects, Chem. Eur. J. 16 (2010) 14094–14105.
[13] M. Wittmann, A. Penzkofer, Concentration-dependent absorption and emission behavior of Sulforhodamine-B in ethylene-glycol, Chem. Phys. 72 (1993) 339–348.
[14] A. Tagaya, S. Teramoto, E. Nihei, K. Sasaki, Y. Koike, High-power and high-gain organic dye-doped polymer optical fiber amplifiers: novel techniques for preparation and spectral investigation, Appl. Opt. 36 (1997) 572–578.
[15] T. Tanaka, K. Yamaguchi, S. Yamamoto, Rhodamine-B-doped and Au (III)–doped PMMA film for three-dimensional multi-layered optical memory, Opt. Commun. 212 (2002) 45–50.
[16] T.-L. Chang, H.C. Cheng, effects on the photoisomerization rates of the zwitterionic and the cationic forms of Rhodamine-B in protic solvents, J. Phys. Chem. 96 (1992) 4874–4878.
[17] F. López Arbeloa, T. López Arbeloa, M.J.T. Estevez, I. López Arbeloa, Photophysics of Rhodamine: molecular structure and solvent effects, J. Phys. Chem. 95 (1991) 2203–2208.
[18] D. Magde, G.E. Rojas, P.G. Seybold, Solvent dependence of the fluorescence lifetimes of xanthenes dyes, Photochem. Photobiol. 70 (1999) 737–744.
[19] K.H. Drexhage, Dye Lasers, second ed., Springer-Verlag, New York, 1977.
[20] T. Karstens, K. Kobs, Rhodamine-B and Rhodamine-101 as reference substances for fluorescence quantum yield measurements, J. Phys. Chem. 84 (1980) 1871–1872.
[21] F.L. Arbeloa, P.R. Ojeda, I.L. Arbeloa, Fluorescence self-quenching of the molecular-forms of Rhodamine-B in aqueous and ethanolic solutions, J. Lumin. 44 (1989) 105–112.
[22] T.L. Chang, W.L. Borst, Effect of solvent polarity on a rotational isomerization mechanism of Rhodamine-B in normal alcohols, J. Chem. Phys. 93 (1990) 4724–4729.
[23] G.B. Dutt, S. Doraiswamy, N. Periasamy, B. Venkataraman, Rotational reorientation dynamics of polar dye molecular probes by picoseconds laser spectroscopic technique, J. Chem. Phys. 93 (1990) 8498–8513.
[24] K.G. Casey, Y. Onganer, E.L. Quitevis, Effect of solvent polarity on nonradiative processes in xanthenes dyes—the acid form of Rhodamine-B in nitrile solvents, J. Photochem. Photobiol. A: Chem. 64 (1992) 307–314.
[25] P. Meallier, M. Moullet, S. Guittonneau, F. Chabaud, P. Chevrou, C. Niemann, Photochemistry of Rhodamine 610, Dyes Pigments 36 (1998) 161–167.
[26] T. Nedelcev, D. Racko, I. Krupa, Preparation and characterization of a new derivative of Rhodamine B with an alkowysilane moiety, Dyes Pigments 76 (2008) 550–556.
[27] A.D. Osborne, A.C. Winkworth, Viscosity-dependent internal-conversion in an aryl-substituted Rhodamine dye, Chem. Phys. Lett. 85 (1992) 513–517.
[28] R.S. Moog, M.D. Ediger, S.G. Boxer, M.D. Fayer, Viscosity dependence of the rotational reorientation of Rhodamine-B in mono-alcohol and poly-alcohol—picosecond transient grating experiments, J. Phys. Chem. 86 (1982) 4694–4700.
[29] A.V. Deshpande, E.B. Namdas, Lasing action of Rhodamine B in polyacrylic acid films, Appl. Phys. B 64 (1997) 419–422.
[30] J.W. Gilliland, K. Yokoyama, W.T. Yip, Solvent effect on mobility and photostability of organic dyes embedded inside silica sol–gel thin films, Chem. Mater. 17 (2005) 6702–6712.
[31] J.W. Gilliland, K. Yokoyama, W.T. Yip, Comparative study of guest charge–charge interactions within silica sol–gel, J. Phys. Chem. B 109 (2005) 4816–4823.
[32] J.M. Drake, R.I. Morse, R.N. Steppel, D. Young, Kiton Red-S and Rhodamine-B—spectroscopy and laser performance of red laser dyes, Chem. Phys. Lett. 35 (1975) 181–188.
[33] P.C. Beaumont, D.G. Johnson, B.J. Parsons, Laser flash photolysis studies of some rhodamine dyes—characterisation of the lowest excited singlet state of Rhodamine 3B, Sulforhodamine B and Sulforhodamine 101, J. Chem. Soc. Faraday Trans. 94 (1998) 195–199.
[34] A.V. Deshpande, E.B. Namdas, Correlation between lasing and photophysical performance of dyes in polymethalmethacrylate, J. Lumin. 91 (2000) 25–31.
[35] S. Sinha, A.K. Ray, S. Kundu, S. Sasikumar, S.K.S. Nair, K. Dasgupta, Photostability of laser dye solutions under copper-vapour-laser excitation, Appl. Phys. B 72 (2001) 617–621.
[36] A. Costela, I. García-Moreno, R. Sastre, Materials for solid-state dye lasers, in: H.S. Nalwa (Ed.), Handbook of Advanced Electronic and Photonic Materials and Devices, vol. 7, Academic Press, New York, 2001, pp. 161–205, Chap. 4.
[37] S. Schultheiss, E. Yariv, R. Reisfeld, H.D. Breuer, Solid state dye lasers: rhodamines in silica–zirconia materials, Photochem. Photobiol. Sci. 1 (2002) 320–323.
[38] S. Sinha, A.K. Ray, S. Kundu, S. Sasikumar, K. Dasgupta, Heavy-water-based solutions of rhodamine dyes: photophysical properties and laser operation, Appl. Phys. B 75 (2002) 85–90.
[39] M. Ahmad, T.A. King, D.-K. Ko, B.H. Cha, J. Lee, Performance and photostability of xanthenes and pyrromethene laser dyes in sol–gel phases, J. Phys. D 35 (2002) 1473–1476.
[40] M. Fukuda, K. Kodama, H. Yamamoto, K. Mito, Evaluation of new organic pigments as laser-active media for a solid-state dye laser, Dyes Pigments 63 (2004) 115–125.
[41] J.D. Badjic, N.M. Kostic, Effects of encapsulation in sol–gel silica glass on esterase activity, conformational stability, and unfolding of bovine carbonic anhydrase II, Chem. Mater. 11 (1999) 3671–3679.
[42] K.K. Flora, J.D. Brenna, Effect of matrix aging on the behavior of human serum albumin entrapped in a tetraethyl orthosilicate-derived glass, Chem. Mater. 13 (2001) 4170–4179.

[43] D.T. Nguyen, M. Smit, B. Duna, J.I. Zink, Stabilization of creatine kinase encapsulated in silicate sol–gel materials and unusual temperature effects on its activity, Chem. Mater. 14 (2002) 4300–4306.
[44] M. Álvarez, F. Amat-Guerri, A. Costela, I. García-Moreno, C. Gómez, M. Liras, R. Sastre, Linear and cross-linked polymeric solid-state dye lasers based on 8-substituted alkyl analogues of pyrromethene 567, Appl. Phys. B. 80 (2005) 993–1006.
[45] M. Rodríguez, A. Costela, I. García-Moreno, F. Florido, J.M. Figuera, R. Sastre, A simple rotating system to avoid early degradation of solid-state dye–lasers, Meas. Sci. Technol. 9 (1995) 971–978.
[46] I. Shoshan, N.N. Danon, U.P. Oppenheim, Narrowband operation of a pulsed dye laser without intracavity beam expansion, J. Appl. Phys. 48 (1977) 4495–4497.
[47] I. López Arbeloa, Fluorescence quantum yield evaluation—corrections for reabsorption and re-emission, J. Photochem. 14 (1980) 97–105.
[48] I. López Arbeloa, K.K. Rohatgi-Mukherjee, Solvent effect on photophysics of the molecular-forms of Rhodamine-B—solvation models and spectroscopic parameters, Chem. Phys. Lett. 128 (1986) 474–479.
[49] T. Nu, G. Liu, J. Zhao, H. Hidaka, N. Serpone, Photoassisted degradation of dye pollutants. V. Self-photosensitized oxidative transformation of Rhodamine B under visible light irradiation in aqueous TiO_2 dispersions, J. Phys. Chem. B 102 (1998) 5845–5851.
[50] G. Liu, X. Li, J. Zhao, H. Hidaka, N. Serpone, Photooxidation pathway of Sulforhodamine-B. Dependence on the adsorption mode on TiO_2 exposed to visible light radiation, Environ. Sci. Technol. 34 (2000) 3982–3990.
[51] C. Chen, W. Zhao, J. Li, J. Zhao, H. Hidaka, N. Serpone, Formation and identification of intermediates in the visible-light-assisted photodegradation of Sulforhodamine-B in aqueous TiO_2 dispersion, Environ. Sci. Technol. 36 (2002) 3604–3611.
[52] N.N. Barashkov, O.A. Gonder, Fluorescence Polymers, Ellis Horwood, Chichester, England, 1994.
[53] A. Costela, I. García-Moreno, D. Del Agua, O. García, R. Sastre, Silicon-containing organic matrices as hosts for highly photostable solid-state dye lasers, Appl. Phys. Lett. 85 (2004) 2160–2162.
[54] A. Costela, I. García-Moreno, D. Del Agua, O. García, R. Sastre, Highly photostable solid-state lasers based on silicon-modified organic matrices, J. Appl. Phys. 101 (2007) 073110.
[55] M. Seydack, Nanoparticle labels in immunosensing using optical detection methods, Biosens. Bioelectron. 20 (2005) 2454–2469.
[56] A. Burns, H. Ow, U. Wiesner, Fluorescent core–shell silica nanoparticles: towards "Lab on a Particle" architectures for nanobiotechnology, Chem. Soc. Rev. 35 (2006) 1028–1042.
[57] J.L. Yan, M.C. Estevez, J.E. Smith, K.M. Wang, X.X. He, L. Wang, W.H. Tan, Dye-doped nanoparticles for bioanalysis, Nano Today 2 (2007) 44–50.
[58] T.T. Morgan, H.S. Muddana, E.I. Altinoglu, S.M. Rouse, A. Tabakovic, T. Tabouillot, T.J. Russin, S.S. Shanmugavelandy, P.J. Butler, P.C. Eklun, J.K. Yun, M. Kester, J.H. Adair, Encapsulation of organic molecules in calcium phosphate nanocomposite particles for intracellular imaging and drug delivery, Nano Lett. 8 (2008) 4108–4115.
[59] C.P.Y. Chan, Y. Bruemmel, M. Seydack, K.K. Sin, L.W. Wong, E. Merisko-Liversidge, D. Trau, R. Renneberg, Nanocrystal biolabels with releasable fluorophores for immunoassays, Anal. Chem. 76 (2004) 3638–3645.
[60] P. Sharma, S. Brown, G. Walter, S. Santra, B. Moudgil, Nanoparticles for bioimaging, Adv. Colloid Interface Sci. 123–126 (2006) 471–485.
[61] O.S. Wolfbeis, Materials for fluorescence-based optical chemical sensors, J. Mater. Chem. 15 (2005) 2657–2669.
[62] J. Widengren, A. Chmyrov, C. Eggeling, P. Löfdahl, C.A.M. Seidel, Strategies to improve photostabilities in ultrasensitive fluorescence spectroscopy, J. Phys. Chem. A 111 (2007) 429–440.
[63] R. Baumann, C. Ferrante, F.W. Deeg, C. Braucle, Solvation dynamics of nile blue in ethanol confined in porous sol–gel glasses, J. Chem. Phys. 114 (2001) 5781–5791.
[64] M.L. Ferrer, F. Del Monte, Study of the adsorption process of Sulforhodamine B on the internal surface of porous sol–gel silica glasses through fluorescence means, Langmuir 19 (2003) 650–653.
[65] A. Tyagi, D. Del Agua, A. Penzkofer, O. García, R. Sastre, A. Costela, I. García-Moreno, Photophysical characterization of pyrromethene 597 laser dye in cross-linked silicon containing organic copolymers, Chem. Phys. 342 (2007) 201–214.